

Exciton-phonon scattering and photo-excitation dynamics in J-aggregate microcavities.

Paolo Michetti

Dipartimento di Fisica, Università di Pisa, Largo Bruno Pontecorvo 3, 56127 Pisa, Italy

Giuseppe C. La Rocca

Scuola Normale Superiore and CNISM Piazza dei Cavalieri 7, 56126 Pisa, Italy

We have developed a model accounting for the photo-excitation dynamics and the photoluminescence of strongly coupled J-aggregate microcavities. Our model is based on a description of the J-aggregate film as a disordered Frenkel exciton system in which relaxation occurs due to the presence of a thermal bath of molecular vibrations. In a strongly coupled microcavity exciton-polaritons are formed, mixing superradiant excitons and cavity photons. The calculation of the microcavity steady-state photoluminescence, following a CW non resonant pumping, is carried out. The experimental photoluminescence intensity ratio between upper and lower polariton branches is accurately reproduced. In particular both thermal activation of the photoluminescence intensity ratio and its Rabi splitting dependence are a consequence of the bottleneck in the relaxation, occurring at the bottom of the excitonic reservoir. The effects due to radiative channels of decay of excitons and to the presence of a particular set of discrete optical molecular vibrations active in relaxation processes are investigated.

PACS numbers: 78.66.Qn, 71.36.+c, 78.20.Bh, 71.35.Aa

Keywords:

I. INTRODUCTION

Strong coupling in solid state microcavities (MCs), has been exhaustively studied in inorganic quantum well devices¹. In these structures Wannier excitons and photon cavity modes are mixed in coherent excitations, called polaritons. A number of interesting phenomena, due to the mixed nature of such eigenstates, such as the parametric processes² and non-equilibrium polariton condensation³, were revealed.

On the other hand, organic strongly coupled MCs have been developed since 1998⁴, by using different kinds of optically active organic layers, among which the cyanine dye J-aggregate films are probably the most typical. Organic materials possess Frenkel excitons, instead of Wannier ones, with large binding energy and oscillator strength. Because of this, organic MCs allow obtaining values of the Rabi splitting up to 300 meV⁵ and offer the possibility of easily observing polaritons at room temperature⁶. Electroluminescence was demonstrated in a J-aggregate strongly coupled microcavity LED⁷ at room temperature. Peculiar molecular phenomena, like the observation of strongly coupled vibronic replicas have also been demonstrated^{8,9}. A detailed review about organic MCs can be found in Refs.^{10,11}

The nature of polaritons in disordered organic MCs has been addressed from the theoretical point of view^{12,13,14,15}, showing the coexistence of delocalized and partially localized polaritons. The possible interaction with molecular vibrations was discussed^{16,17}, the effect of anisotropy in organic crystal was characterized¹⁸, as well as the possible occurrence of non-linear phenomena¹⁹ for high density of polaritons.

We believe that, as in the case of inorganic MCs, theoretical efforts towards a qualitative, but also quantitative, understanding of the relaxation processes in organic MC dynamics are an essential support to the work of experimental teams involved in the study of organic microcavities, in principle able to give rise to a rich variety of phenomena, similar to what obtained with their inorganic counterpart and more, thanks to the infinite possibilities of organic chemistry. A recent model described the dynamics of a J-aggregate MC due to the strong coupling of polariton with optical molecular vibrations²⁰ through the application of a quantum kinetic theory. Our approach¹⁷, even though restricted to a rate equation description of the relaxation processes, allows for a more flexible and complete description of the physical system at hand, accounting for the photoluminescence of a 2D MC starting from an accurate description of the bare active material (the J-aggregate film). Besides we are also able to perform time dependent simulations of J-aggregate microcavity photoluminescence²¹ and estimate their radiative decay time in linear pumping regime. In particular, we here extend our model, which includes the presence of a large number of weakly coupled excitons, considering the occurrence of a radiative relaxation channel from such excitons to the cavity polaritons, as first suggested in ref.²². We also include the effects on the polariton relaxation due to the presence of a discrete spectrum of molecular vibrations, as in²⁰, which however are here supposed to scatter weakly with the electronic excitations without taking part directly in the cavity-polariton formation.

II. THE MODEL

A J-aggregate can be thought as a chain of N_d dye molecules linked by electrostatic interactions. Its excitations are described by the Frenkel Hamiltonian:

$$H = \sum_i E_i b_i^\dagger b_i + \sum_{i \neq j} V_{ij} (b_i^\dagger b_j + b_j^\dagger b_i) \quad (1)$$

where b_i^\dagger are the monomer exciton creation operators, corresponding to Gaussian distributed energies E_i , with standard deviation σ , to account for static disorder. The hopping term is given by $V_{ij} = J = J_0 \frac{1}{|i-j|^\beta}$ where $J > 0$ is the nearest neighbor coupling strength. The eigenstates are found by direct diagonalization of the Frenkel Hamiltonian and are described by the operators $B^\nu = \sum_i c_i^{(\nu)} b_i^\dagger$, where c_i is the coefficient of the i -th exciton on the i -th monomer. The oscillator strength of each state is given by $F = \sum_i |c_i^{(\nu)}|^2$, with $\sum_\nu F = N_d$, having the molecules equal transition dipole and being the wavelength much greater than the aggregate length. The excitations are delocalized Frenkel excitons with an energy dispersion curve, called the J band, where most part of the aggregate oscillator strength is concentrated on the superradiant bottom states²³. Higher energy excitons very weakly couple with light. While the hopping term determines the formation of the J band, static disorder gives rise to a low energy tail in the exciton DOS, corresponding to partially localized, inhomogeneously broadened, superradiant eigenstates, responsible of the luminescence and, in MCs, of the strong light-matter coupling.

Delocalized polaritons are the result of the strong light-matter interaction between such superradiant excitons, localized on each aggregate, and the photon cavity modes, ideally extended over the whole structure. To treat the MC case we include a model polariton wavefunction of wavevector k , linking the J aggregate excitons into the polariton states¹⁷. The total exciton and photon fraction, $C_k^{(ex)}$; $C_k^{(ph)}$, and the polariton dispersion curve $E_{JL}(k)$ are given by the usual two coupled oscillator model. The modulus of the exciton coefficients $c_{iI}^{(k)}$, describing how each exciton of I -th aggregate participates in the polariton states, are the only relevant quantities entering our model. We consider the polaritons to be extended with equal degree on each one of the N_{agg} aggregates and make the assumption that the weight of each exciton in the polariton states is proportional to its oscillator strength, so that $\sum_I |c_{iI}^{(k)}|^2 = \frac{F}{N_d}$.

In organic microcavities the strong coupling region, where polaritons do form, is typically extended till about $q_{max} = 10^5 \text{ cm}^{-1}$, where the Bragg mirrors stop-band starts to fail, or is also more restricted by inhomogeneous disorder^{12,15}. Therefore the excitation spectrum is composed, besides polaritons, of a number of uncoupled molecular excitons that form an excitonic reservoir (ER)^{12,15,16} as shown in Fig.1. The excitonic part of the polaritons are formed by a Bloch sum, with $q < q_{max}$, made from the superradiant molecular excitons of the J-aggregates, while the ER is composed by uncoupled superradiant excitons from the remaining part of the Brillouin zone, plus a number of higher energy "dark" excitons. We note that the ratio between polaritons and uncoupled excitons of the ER can be of the order of $(q_{max} R)^{-1} N_d^{-1} 10^{-3}$ or less.

The dynamics of the system is described by rate equations for the population $f_i(t)$ of the state i , including the scattering rates, due to a weak linear exciton-phonon coupling, among all the kinds of particles present in the system which have a non-null exciton component. Dealing with a 2D microcavity, we assume isotropic conditions, in which the polariton population only depends on the modulus of the wavevector, in order to reduce the dimensionality of the problem. We consider localized vibrations, that can be due to the molecules itself or to the local environment, located on each chain site with a continuous spectrum, choice that follows literature reports^{24,25} on J-aggregate simulations. We will address this model as the continuous spectrum of vibration (CSV) model. We also extend the model to account for a series of discrete optical vibrations in what we will refer as the discrete vibrations model (DV model), such specific modes can be of particular relevance when their energy is nearly resonant with the Rabi splitting^{20,22}. In particular the DV model includes a continuum of vibrations for energy below 25 meV and two discrete molecular vibrations of $E_1 = 40 \text{ meV}$ and $E_2 = 75 \text{ meV}$, with an exciton-phonon coupling factor $g_1 = 0.4$ and $g_2 = 0.5$, respectively. The values of the molecular vibrations are chosen following the Ram an experiments on J-aggregate films, as reported in²⁰.

The scattering rates from the state i to the i^0 , which can either be an exciton $i = n = (j; I)$, the j -th exciton of the I -th aggregate, or a delocalized polariton of wavevector k , can be expressed in an unique compact notation. If we consider the interaction with a continuous spectrum of vibrations, for which the vibrational DOS is non-zero for any energy difference $E = E_{i^0} - E_i$ between final and initial state, we adopt the following expression

$$W_{i^0, i} = W_0 \frac{1}{|i - i^0|^\beta} (N_{j, E} + \theta(E)) \frac{j E j^\beta}{J} \quad (2)$$

where W_0 and β are parameters related to the exciton-photon interaction energy and to the shape of the vibration spectrum, $N_{j, E}$ is the Bose-Einstein occupation factor, $\theta(E)$ the step function. If we instead consider the interaction

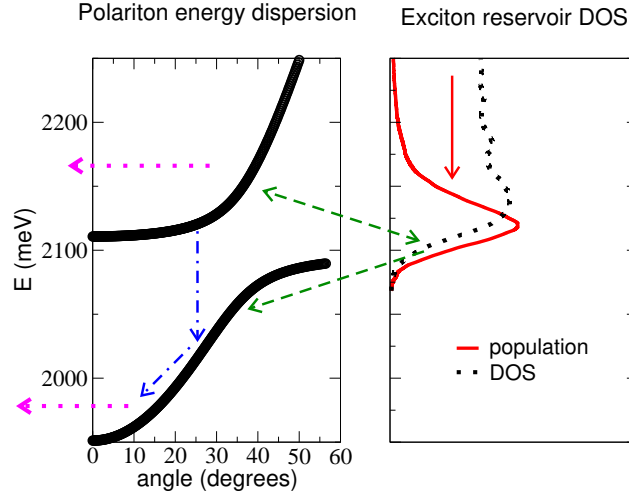


FIG. 1: (Color online) On the left polariton dispersion curves for $\hbar\omega = 80$ meV, on the right the exciton reservoir DOS (dotted line) and steady state population (continuous line) are represented. The possible scattering mechanisms are sketched out: exciton to exciton (continuous arrow), exciton to/from polariton (dashed arrow), polariton to polariton (dotted-dashed arrow), polariton radiative decay (dotted arrow).

with a molecular vibration of discrete energy E_{vib} we obtain

$$W_{i^0;i} = \frac{2}{\hbar} \frac{g^2 E_{vib}^2}{\omega_{i^0}} \sum_j (N_j \delta(E_j + E_{vib}) - \delta(E_j - E_{vib})) \quad (3)$$

where $\delta(E)$ is the Dirac delta and g the exciton-phonon coupling parameter for the vibration of energy E_{vib} . What distinguishes the different processes is the overlap factor ω_{i^0} . In fact the emission or absorption of localized vibrations promotes the scattering among states that have an exciton participation on the same molecular site. Therefore the factor ω_{i^0} takes into account of the partial exciton nature of polaritons, of their delocalized nature and are proportional to an excitonic overlap factor I obtained by carrying out the sum of the excitonic participation of the initial and final state on each molecular site. The overlap factor is one of the following:

$$I_{i^0;i} = I_i I_{i^0}; \quad (4)$$

$$I_{k;n^0} = \frac{D(k) \mathcal{F}_k^{(ex)} \mathcal{F}_n^{(ex)}}{N_{agg}} I_{n^0}^{(ex \text{ pol})} \quad (5)$$

$$I_{n^0;k} = \frac{\mathcal{F}_k^{(ex)} \mathcal{F}_n^{(ex)}}{N_{agg}} I_{n^0}^{(ex \text{ pol})} \quad (6)$$

$$I_{k^0;k} = \frac{D(k^0) \mathcal{F}_{k^0}^{(ex)} \mathcal{F}_k^{(ex)}}{N_{agg}^2} I^{(p \text{ p})} \quad (7)$$

respectively, in the case of scattering from an exciton to another exciton ($i = n, i^0 = n^0$), where $I_{i^0;i}$ is the excitonic overlap factor; or for the scattering from an exciton n^0 to a polariton k , with $I_{n^0}^{ex \text{ pol}}$ their excitonic overlap factor, and $D(k)$ the number of states corresponding, in the inverse space grid, to the polariton variable of modulus wavevector k ; or when describing the opposite process ($i = k, i^0 = n^0$); or in the latter case of scattering between two polaritons, where $I^{(p \text{ p})}$ is an excitonic overlap factor between polaritons (the derivation of the rates can be found in Ref.¹⁷).

We also add a radiative channel of decay from the ER to the polaritons, accounting for the presence in the MC of a fraction of excitons weakly coupled with light. In fact, inside a strongly coupled cavity a fraction of weakly coupled excitons can decay radiatively pumping the photonic part of polaritons²². We model the spontaneous emission of polaritons from the ER similar to the bare luminescence times a switching factor:

$$W_{k^0;k}^{rad} = \frac{D(k) \mathcal{F}_k^{(ph)} \mathcal{F}_k^{(ph)}}{D(k^0) \mathcal{F}_{k^0}^{(ph)} \mathcal{F}_{k^0}^{(ph)}} g(E_k); \quad (8)$$

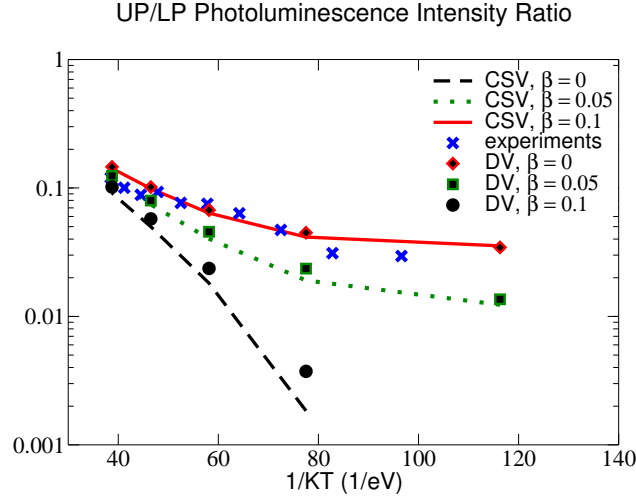


FIG. 2: (Color online) The C ratio as a function of temperature for a MC with $\epsilon = 130$ meV. The experimental results from Ref.²⁷ (X marks) are compared with simulations with increasing importance of the radiative channel $\epsilon_{\text{rad}} = 0, 0.05$, and 0.1 , for both the model with continuous spectrum of vibrations and the model DV model.

the contribution of the excitons is proportional to the bare exciton luminescence ratio ϵ_{rad} , the transfer matches energy conservation, while the normalization is chosen to obtain a net exciton radiative decay towards polaritons of times the spontaneous emission (ϵ_{rad}). g is a Lorentzian shape broadening function, where the energy uncertainty is given by the finite particle lifetime.

The damping rate of polaritons, due to photon escape through the cavity mirrors, is given by $\gamma_i = \mathcal{F}_i^{(\text{ph})} \gamma = \frac{1}{\tau_i}$, where typically $\tau_i = 35$ fs. For the upper and lower polaritons we consider the reciprocal space up to $q_{\text{max}} = 9 \times 10^4 \text{ cm}^{-1}$, discretized in a grid of 280 points. The effect of the inhomogeneous disorder are taken in account averaging the scattering rates over an ensemble of 10^3 J-aggregates each having $N_d = 100$ monomers. The dyes hopping energy is fixed at $J = 75$ meV, and the dye spontaneous emission lifetime is $\tau_0 = 0.33 \text{ ns}^{-1}$; while the parameters $\epsilon = 0.54J$, $p = 0.8$ and $W_0 = 3.2J = \hbar$, have been fixed in order to obtain the best fit the bare J-aggregate luminescence and emission features¹⁷.

III. PHOTOLUMINESCENCE SIMULATION

A. Continuous spectrum of vibrations

Solving the rate equations for the J-aggregate microcavity, with the same procedure described in ref.¹⁷, we obtain the polariton steady state population, from which we calculate the angle resolved photoluminescence, by imposing the conservation of energy and in-plane momentum between cavity-polaritons and external photons. For both the CSV and the DV models, we draw the indication that the major part of the population is frozen on the ER. The origin of this bottleneck is due essentially to three reasons: the small number of polariton states with respect to the ER ones, second the interaction between a localized vibration and a polariton is reduced by the delocalized, and mixed, nature of exciton-polaritons, in fact the scattering rates scale as $1/N_{\text{coher}}$, where N_{coher} is the number molecular sites over which the polariton is delocalized. Third is the small photon lifetime, due to the low quality factor of organic MCs. The photoluminescence can be thought of as the result of the escape through the cavity mirrors of a particle, following the previous scattering on the polariton branches from the ER, with the absorption or emission of a vibrational quantum.

In Fig.1 we draw a sketch of the excited states on a J-aggregate microcavity and of the possible scattering processes following non resonant pumping. In particular we stress that the relaxation inside a J-aggregate is faster than ER to polariton scattering and leads to a steady state population (shown in the right figure in continuous line), from which polariton pumping occurs. The ER DOS is inhomogeneously broadened by static disorder and ER steady state population is similar to that of a non-cavity sample. We note here that the average difference between the energy of the steady state population and the luminescence maximum results to be about $\epsilon = 15$ meV.

An experimentally accessible parameter, used to analyze the effectiveness of relaxation in organic microcavities, is the photoluminescence intensity ratio $C = \frac{UPL}{LPL}$ recorded at resonance angle, where polariton branches

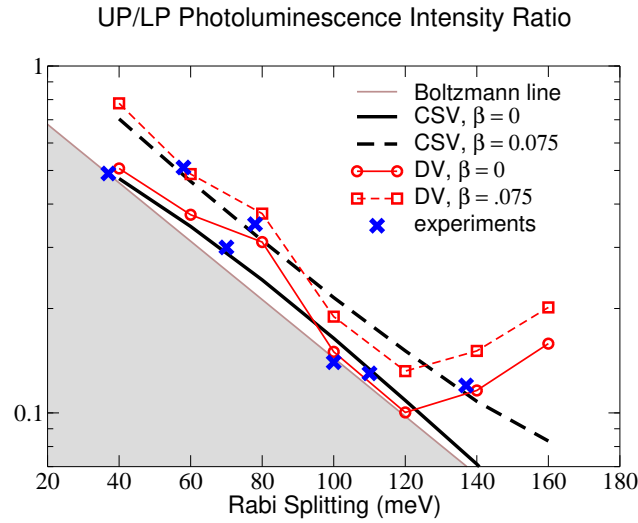


FIG. 3: (Color online) The C ratio as function of the Rabi splitting for microcavities with $\gamma = 0$ and $\gamma = 0.075$, for the models with continuous and discrete spectrum of vibrations. The calculation are compared with the experimental data in blue 'x's'²⁰.

are half matter and half light, and their energy distance from the exciton resonance is half the Rabi splitting ($\omega = 2$). We focus on the temperature dependence of the C ratio between 50 and 300 K for a MC with a Rabi splitting of $\omega = 130$ meV, shown in Fig. 2, and compare it with the experimental result reported by D.G. Lidzey's group²⁷. With $\gamma_{\text{rad}} = 0$ the C ratio shows a smooth thermal activation, but it is difficult to get any UP PL at low temperature. This is consistent with the fact that UP PL follow the absorption of a vibrational quantum from a particle at the bottom of the ER and therefore is proportional to number of vibrations (varying as a Boltzmann factor). Turning on the radiative channel ($\gamma_{\text{rad}} > 0$), being it independent on temperature, we obtain a low temperature saturation of the UP PL and the C ratio exhibits a plateau as experimentally found^{26,27}. The experimental data are well reproduced and stay between the simulations with $\gamma_{\text{rad}} = 0.05$ and $\gamma_{\text{rad}} = 0.1$.

We also show in Fig. 3 the simulation of the C ratio as a function of the Rabi splitting in comparison with experimental data from Ref.²⁰. Increasing the Rabi splitting value reduces the probability for a particle in the ER to be scattered on the UP branch, because such process would need the absorption of a vibration of greater energy from the thermal bath. The data therefore roughly follows a Boltzmann factor $e^{-\frac{\omega}{2k_B T}}$, shown for comparison, where $\omega = 2$ corresponds, at resonance angle, to the energy separation from the ER bottom and the UP and LP states. With a continuous vibrational spectrum we observe the smooth Boltzmann behavior, while the inclusion of the radiative channel rigidly shifts the C ratio toward higher values. The experimental data (blue X symbols) stay in between the simulation performed without the radiative channel $\gamma_{\text{rad}} = 0$ and the simulation with the radiative process turned on with $\gamma_{\text{rad}} = 0.075$.

B. Model with discrete vibrations

The temperature dependence of the C ratio, shown in Fig. 2 is largely unaffected by the introduction of the discrete spectrum of vibration and the same considerations as for the CSV case still apply. If we instead consider the Rabi splitting dependence, the inclusion of discrete energy vibrations leads to the fluctuation of the C ratio and to a deviation from the smooth Boltzmann-like behavior. In particular the DV model reproduces the drop in the C factor between 80 to 100 meV, associated with $\omega = 2 \approx 40$ meV and the activation of the UP depletion towards the ER bottom with emission of a vibrational quantum and permits to obtain a better fit of experimental data. We believe that the agreement we obtain with the available data as show in Fig. 3 is of comparable quality to that obtained by Chovan et al.²⁰. Of course, this is not to say that the phonon strong coupling approach they consider is immaterial. It is plausible that also in J-aggregate microcavities exciton and molecular vibrations may interact strongly leading to non perturbative effects^{8,9,28} such as, in particular, the formation of cavity polaritons with the concomitant participation of optical phonon, exciton and cavity photon modes, a phenomenon which has also been considered in bulk semiconductors (see the concept of "phononiton"²⁹). It remains to be seen, however, whether there is as yet a compelling experimental evidence for the occurrence of such a phonon strong coupling in J-aggregate microcavities, the photoluminescence of which is here considered.

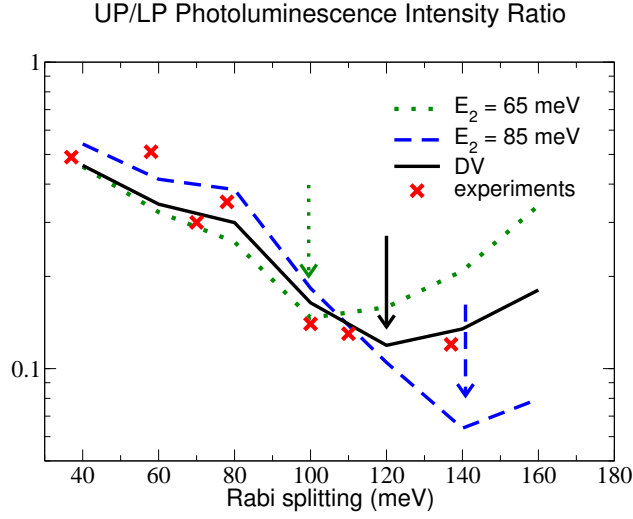


FIG. 4: (Color online) C ratio as function of the Rabi splitting for microcavities with $\gamma = 0$, for the DV model ($E_2 = 75$ meV) in continuous line, with E_2 changed in 65 meV (dotted line), with $E_2 = 85$ meV (dashed line). The calculation are compared with the experimental data in blue 'x's²⁰.

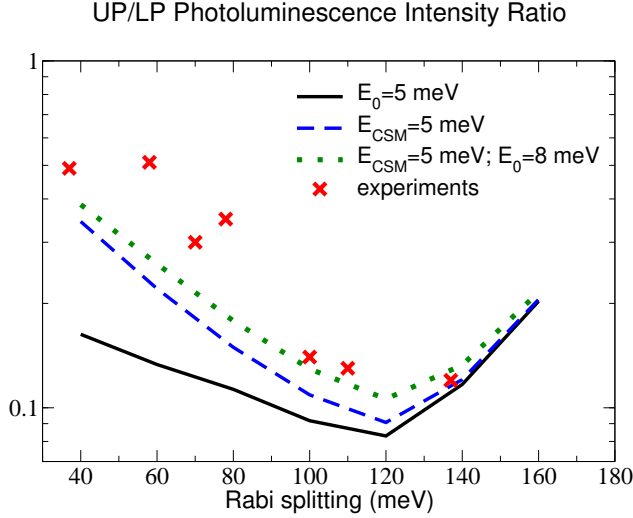


FIG. 5: (Color online) C ratio as function of the Rabi splitting for microcavities with $\gamma = 0$ and low energy vibrational spectrum modified with respect to the DV model. Simulation with no CSV and a defined energy vibration $E_0 = 5$ meV (continuous line); with $E_{CSM} = 5$ meV (dashed); with $E_{CSM} = 5$ meV, plus a defined energy vibration $E_0 = 8$ meV (dotted). The calculation are compared with the experimental data in blue 'x's²⁰.

Apart for the particular choice of the definite energy vibrations we made in the DV model ($E_{CSM} = 25$ meV, $E_1 = 40$ meV, $E_2 = 75$ meV), we also tested different sets of optical vibrations in order to understand their effects on the C ratio as a function of the Rabi splitting. In general it is not possible to completely distinguish the individual effects of each one of E_{CSM} , E_1 , E_2 , however we are able to identify some trends.

Firstly we analyze the role of optical vibration E_2 by increasing it from 65 meV to 85 meV. As shown in Fig. 4 a minimum is observed at different Rabi splitting for different values of E_2 . The motivation is that the ER to LP scattering rate is in resonance when $E_{ER} \approx E_{LP} \approx E_2$, with E_{ER} averaged on the steady state population of the exciton reservoir. When the process is in full resonance we expect a minimum of the C factor, as it is evidenced in Fig. 4. Following this rule we expect the minimum to be located in $\Omega_{min} = 2(E_2 - \gamma)$. Because of the different position of Ω_{min} , when ER to LP scattering is maximum, for small Rabi splitting the C factor decreases with E_2 , while we find the opposite behavior for Ω greater than 100 meV. As we will see, the occurrence of the C minimum depends on the presence of higher energy vibrations active in relaxation processes, here not included.

We now focus on the role of the low energy vibrations. Initially we modify the DV model including the single

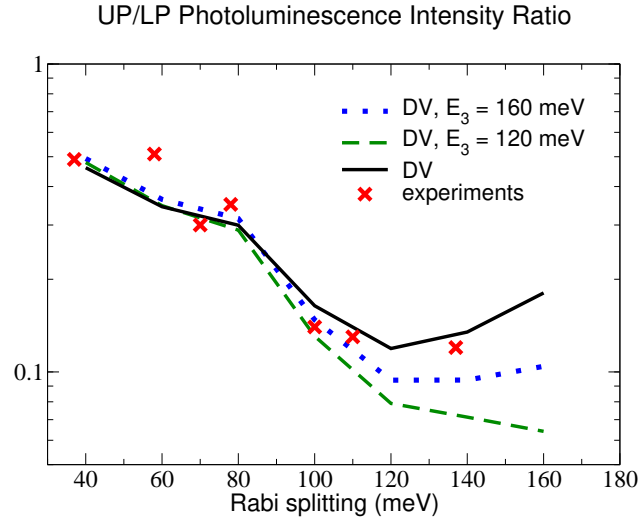


FIG. 6: (Color online) C ratio as function of the Rabi splitting for microcavities with $\gamma = 0$, for the DV model plus an high energy vibration $E_3 = 120$ (dotted), 160 meV (dashed). The calculation are compared with the experimental data in blue \times S^{20} .

vibration $E_0 = 5$ meV instead of the continuous spectrum of low energy vibrations. The result, in Fig.5, is a significant reduction of the C factor for γ smaller than 120 meV. We can understand this if we consider that UP population is mainly due to the ER to UP scattering, that takes place from steady state ER population with absorption of a molecular vibration, while the direct relaxation in UP from high energy excitons gives a minor contribution. This process involving absorption of a vibrations is active at room temperature till around $E_0 = k_B T$ (if the vibrational DOS is not zero), therefore it is significant for UP energies equal to the mean ER population energy ($\bar{\epsilon}$) plus $k_B T$, that corresponds to Rabi splitting values $< 2(\bar{\epsilon} + k_B T) \approx 80$ meV. Therefore a reduction in the active low energy DOS means a significant reduction of the ER to UP scattering and of the C ratio for small γ . If we modify DV choosing $E_{CSM} = 5$ meV we note that after $\bar{\epsilon} = 2(\bar{\epsilon} + E_{CSM}) = 40$ meV we have a rapid decrease of the C factor and a minimum, as predicted around 120 meV. So it is clear that to recover the experimental data we need a series of active vibrations between 5 and 25 meV.

Finally let's consider the effects of a third optical vibration $E_3 > E_2$, in particular we set $E_3 = 120$ meV or $E_3 = 160$ meV with $g_3 = 0.3$. As can be seen in Fig.6 the presence of E_3 has effects on C only for large enough Rabi splitting, for which $\bar{\epsilon} + 2\gamma$ approach E_3 . For $E_3 = 120$ meV, with γ in the range considered, the non-monotonic behavior of C vanishes correspondent to the fact that the LP is pumped from the ER almost thermalized population with an emission of a vibration E_3 . If we increase E_3 to 160 meV the ER to LP scattering become too much out of resonance to contribute and numerical data are nearer to the DV case. It must be noted that the possible presence of a C minimum is conditioned to the absence of optical vibrations of higher energy E_3 active in relaxation processes.

IV. CONCLUSIONS

In conclusion our model, based on semiclassical rate equations, explains sufficiently well the presently available experimental data on strongly coupled J-aggregate microcavities. In particular, the photoluminescence under non-resonant pumping follows the scattering of an electronic excitation from the ER bottom, where the population is accumulated, towards the polariton branches. Such scattering can either happen with the absorption/emission of vibrational quanta (with a continuous as well as discrete spectrum), process which is sensitive to temperature, or be due to pumping of polaritons by the spontaneous radiative decay of weakly coupled excitons. The interplay between the two processes determines both the specific temperature dependence of the polariton branches photoluminescence intensity ratio and its Rabi splitting dependence.

Electronic address: michetti@df.unipi.it

¹ Edited by B. Deveaud, The Physics of Semiconductor Microcavities, (Wiley-VCH, Weinheim, 2007)

- ² M .Saba, C .C iuti, J .B loch, V .Thierry-M ieg, R .Andre, L .S .D ang, S .K underm ann, A .M ura, G .Bongiovanni, J .L .Staehli, B .D eveaud, *Nature* 414, 731 (2001).
- ³ J .K asprzak, M .Richard, S .K underm ann, A .Baas, P .Jeam brun, J M .J .Keeling, F M .M archetti, M .H .Szym anska, R .Andre, J .L .Staehli, V .Savona, P B .L ittlewood, B .D eveaud, Le SiD ang, *Nature* 443, 409 (2006).
- ⁴ D G .Lidzey, D D C .B radley, M .S .Skolnick, T .V irgili, S .W alker, D M .W hittaker, *Nature* 395, 53 (1998).
- ⁵ P A .Hobson, W L .Barnes, D G .Lidzey, G A .Gehring, D M .W hittaker, M .S .Skolnick, S .W alker, *Appl. Phys. Lett.* 81, 3519 (2002).
- ⁶ D G .Lidzey, D D C .B radley, T .V irgili, A .A m itage, M .S .Skolnick, S .W alker, *Phys. Rev. Lett.* 82, 3316 (1999).
- ⁷ J R .T ischler, M .S .B radley, V .Bulovic, J H .Song, A .Num ikko, *Phys. Rev. Lett.* 95, 036401 (2005).
- ⁸ R .J .H olm es, S R .Forrest, *Phys. Rev. Lett.* 93, 186404 (2004).
- ⁹ L .Fontanesi, G C .La Rocca, *Phys Stat Sol (c)* 5, 2441 (2008)
- ¹⁰ R .J .H olm es, S R .Forrest, *Organic Electronics* 8, 77 (2007).
- ¹¹ D G .Lidzey, in: "Electronic excitations in organic based nanostructures", Eds. V M .A granovich and F .Bassani, *Thin Film s and Nanostructures* vol. 31, (Elsevier, San D iego, 2003) chap. 8.
- ¹² V M .A granovich, M .L itinskaia, D G .Lidzey, *Phys. Rev. B* 67, 085311 (2003).
- ¹³ P .M ichetti, G C .La Rocca, *Phys. Rev. B* 71, 115320 (2005).
- ¹⁴ V M .A granovich, Y N .G artstein, *Phys. Rev. B* 75, 075302 (2007).
- ¹⁵ P .M ichetti, G C .La Rocca, *Physica E* 40, 1926 (2008).
- ¹⁶ M .L itinskaya, P .Reineker, V M .A granovich, *J .Lum in.* 119, 277 (2006).
- ¹⁷ P .M ichetti, G C .La Rocca, *Phys. Rev. B* 77, 195301 (2008).
- ¹⁸ H .Zoubi, G C .La Rocca, *Phys. Rev. B* 71, 235316 (2005).
- ¹⁹ H .Zoubi, G C .La Rocca, *Phys. Rev. B* 72, 125306 (2005).
- ²⁰ J .Chovan, I .E .Perakis, S .Ceccarelli, D G .Lidzey, *Phys. Rev. B* 78 045320 (2008).
- ²¹ P .M ichetti, G .C .La Rocca, *Sol. St. Phys. C*, 1-4 (2008) /D O I 10.1002/pssc.200880310.
- ²² D G .Lidzey, A M .Fox, M D .Rahn, M .S .Skolnick, V M .A granovich, S .W alker, *Phys. Rev. B* 65, 195312 (2002).
- ²³ Edited by T .K obayashi, *J-Aggregates*, (W orld Scienti c, Singapore, 1996).
- ²⁴ M .Bednarz, V A .M alyshev, J .Knoester, *J .Chem .Phys* 117, 6200 (2002).
- ²⁵ D .J .H eij, V A .M alyshev, J .Knoester, *J .Chem .Phys* 123, 144507 (2005).
- ²⁶ P .Schouw ink, J .M .Lupton, H .von Berlepsch, L .D ahne, R F .M ahrt, *Phys.Rev.B* 66, 081203(R) (2002).
- ²⁷ S .Ceccarelli, J .W enus, M .S .Skolnick, D G .Lidzey, *Superlattices and M icrostructures* 41, 289 (2007).
- ²⁸ D .Em briaco, D B .Balagurov, G C .La Rocca, V M .A granovich, *Phys Stat Sol (c)* 1, 1429 (2004)
- ²⁹ A L .Ivanov, L V .K eldysh, *Sov Phys.-JETP* 57, 234 (1982); B S .W ang, J L .B im an, *Phys. Rev. B* 42, 9609 (1990).

UP/LP Photoluminescence Intensity Ratio

